

This article was downloaded by: [Tomsk State University of Control Systems and Radio]

On: 18 February 2013, At: 13:45

Publisher: Taylor & Francis

Informa Ltd Registered in England and Wales Registered Number: 1072954

Registered office: Mortimer House, 37-41 Mortimer Street, London W1T 3JH, UK



## Molecular Crystals and Liquid Crystals Science and Technology. Section A. Molecular Crystals and Liquid Crystals

Publication details, including instructions for authors and subscription information:

<http://www.tandfonline.com/loi/gmcl19>

### Temperature Dependence of the Torsional Anchoring Strength of a Nematic Liquid Crystal, 5CB, Aligned on the Treated Substrates

Takashi Sugiyama<sup>a b</sup>, Seiyu Kuniyasu<sup>a b</sup> & Shunsuke Kobayashi<sup>a</sup>

<sup>a</sup> Division of Electronic and Information Engineering, Faculty of Technology, Tokyo University of Agriculture and Technology, 2-24-16 Nakamachi, Koganei-shi, Tokyo, 184, Japan

<sup>b</sup> Stanley Electric Co. Ltd., 1-3-1 Eda-nishi, Midori-ku, Yokohama-shi, Kanagawa, 225, Japan

Version of record first published: 04 Oct 2006.

To cite this article: Takashi Sugiyama, Seiyu Kuniyasu & Shunsuke Kobayashi (1994): Temperature Dependence of the Torsional Anchoring Strength of a Nematic Liquid Crystal, 5CB, Aligned on the Treated Substrates, Molecular Crystals and Liquid Crystals Science and Technology. Section A. Molecular Crystals and Liquid Crystals, 238:1, 1-11

To link to this article: <http://dx.doi.org/10.1080/10587259408046911>

PLEASE SCROLL DOWN FOR ARTICLE

Full terms and conditions of use: <http://www.tandfonline.com/page/terms-and-conditions>

This article may be used for research, teaching, and private study purposes. Any substantial or systematic reproduction, redistribution, reselling, loan, sub-licensing, systematic supply, or distribution in any form to anyone is expressly forbidden.

The publisher does not give any warranty express or implied or make any representation that the contents will be complete or accurate or up to date. The accuracy of any instructions, formulae, and drug doses should be independently verified with primary sources. The publisher shall not be liable for any loss, actions, claims, proceedings, demand, or costs or damages whatsoever or howsoever caused arising directly or indirectly in connection with or arising out of the use of this material.

# Temperature Dependence of the Torsional Anchoring Strength of a Nematic Liquid Crystal, 5CB, Aligned on the Treated Substrates

TAKASHI SUGIYAMA,<sup>†</sup> SEIYU KUNIYASU,<sup>†</sup> and SHUNSUKE KOBAYASHI

*Division of Electronic and Information Engineering, Faculty of Technology, Tokyo University of Agriculture and Technology, 2-24-16 Nakamachi, Koganei-shi, Tokyo 184, Japan*

*(Received November 16, 1992; in final form March 22, 1993)*

The temperature dependence of the torsional anchoring strength of a nematic liquid crystal (NLC), 5CB, aligned in the cells with orientation layers of rubbed alkylbranched and branchless polyimide (PI) films has been measured. These results are analyzed based on the van der Waals model which assumes that the extrapolation length  $d_e$  consists of two parts:  $d_e(1)$  which is function of both the bulk order parameter and that of the interfacial region; and  $d_e(2)$  which is intrinsic to the surface anchoring. It is shown that  $d_e(1)$  increases slightly with temperature, but  $d_e(2)$  decreases, whereas it increases in a sample with obliquely evaporated SiO films.

**Keywords:** *torsional anchoring strength, temperature dependence, branched polyimide film, branchless polyimide film, bulk order parameter, surface order parameter*

## 1. INTRODUCTION

The surface anchoring of a homogeneously aligned nematic liquid crystal (NLC) disposed in a cell is characterized by polar (off-surface) coupling strength and torsional (azimuthal- on a plane) deformation. A lot of papers have been published on the polar anchoring strengths and their temperature dependence.<sup>1–4</sup> However, only a little research has been conducted and reported on the torsional coupling strength (TCS)  $A\phi$ .<sup>5–6</sup> Among them the present authors reported on TCS, as a function of the pretilt angle for NLC, 5CB, aligned on rubbed films of polyimide (PI) having alkylamine chains as branches that were aligned in an inclined form by performing an appropriate rubbing; the result was analyzed based on a steric interaction between LC molecules and the inclined branches.

The present paper reports on the experimental results of the temperature de-

<sup>†</sup>On leave from Stanley Electric Co. Ltd., 1-3-1 Eda-nishi, Midori-ku, Yokohama-shi, Kanagawa 225, Japan.

pendence of the anchoring strength for an NLC, 5CB, aligned on PI films with and without an alkylbranch. The result is analyzed and explained based on the van der Waals model developed by Yokoyama *et al.*,<sup>1</sup> where the extrapolation length consists of the contribution from the anisotropic interaction at the interface and that from the inhomogeneity of the orientational order parameter profile in the interfacial region. Firstly, we analyzed the temperature dependence of these two contributions from the spatial and temperature variation of the changing of the surface order parameter. Then, secondly, a theoretical evaluation of the torsional anchoring strength was calculated as a function of the shape of the branches, i.e., their angle and length as was done in the previous paper.<sup>5</sup>

For a comparison the investigation has been made on the system of obliquely evaporated SiO and 5CB.

## 2. EXPERIMENTAL METHOD AND DERIVATION OF TORSIONAL ANCHORING STRENGTH

The NLC used in this research was 5CB which were aligned homogeneously on properly prerubbed alkylbranched and branchless PI films in the sandwich cells. For a comparison, other cells containing 5CB aligned on obliquely evaporated SiO films were also prepared. In Table I, the code name of the samples, A through E, and their pretilt angles at low temperature are shown. The pretilt angles were controlled and generated by adjusting the rubbing strength.<sup>7</sup> In all the cells the thickness of the LC layers was 70  $\mu\text{m}$ . The measuring system for the TCS used in this research was the same as that described in a previous paper.<sup>5</sup> The values of  $d_e$  were derived by a theoretical fitting to the data of the transmitted light through the system as a function of the magnetic field, where the variation of the LC molecular conformation with the applied magnetic field was calculated in advance by solving the free energy function for a pretilted NLC medium using the Runge-Kutta method.

## 3. RESULTS

The temperature dependence of the extrapolation length  $d_e$ , for the cells with the branched and branchless polyimide films and those of obliquely evaporated SiO

TABLE I

Sample	Alignment film	Pretilt angle
A	PI (branched)	4.1°
B	PI (branched)	3.1°
C	PI (branchless)	2.1°
D	SiO	0°
E	SiO	0°

are shown in Figure 1. It is found that  $d_e$  of SiO is seen to undergo a nearly diverging increase toward  $T_{NI}$  that is almost analogous to the result obtained by Yokoyama *et al.* for the polar anchoring.<sup>1</sup> But on the contrary to this, in the samples with two kinds of PI films  $d_e$  slightly increases with temperature and does not indicate the diverging behavior. It is also found that the obtained  $d_e$  is smaller for a cell with the branched PI as compared with that of a branchless PI; moreover, that a smaller  $d_e$  is obtained for a cell with a higher pretilt angle as is seen in the data for the samples A and B.

#### 4. DISCUSSION

The fact that the temperature dependence of  $d_e$  for a cell with PI films does not show a nearly diverging increase toward  $T_{NI}$ , which is obtained for the obliquely evaporated SiO, may be understood by the difference in the temperature dependence of the surface order parameter  $S_s$  and that of the bulk  $S_b$ . Based on Yokoyama's analysis,<sup>1</sup>  $d_e$  is divided into two essentially distinct contributions as follows:

$$\begin{aligned} d_e &= d_e(1) + d_e(2) \\ &= d_e(1) + g(\theta_0)/A\phi \end{aligned} \quad (1)$$

$$g(\theta_0) = \cos^2\theta_0(K_{22} \cos^2\theta_0 + K_{33} \sin^2\theta_0),$$

where  $\theta_0$  is the pretilt angle,  $K_{22}$  and  $K_{33}$  are the Frank elastic constants for splay

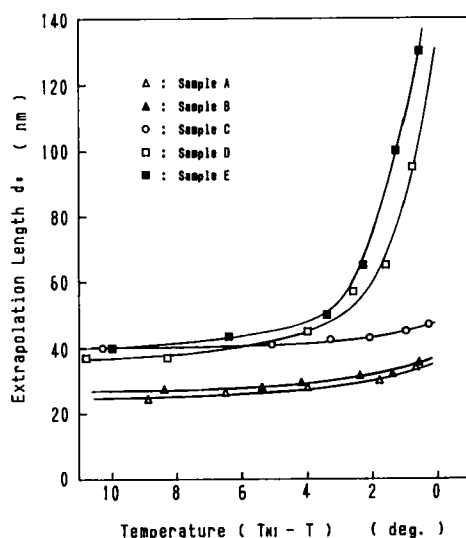


FIGURE 1 Experimental results for the temperature dependence of the extrapolation length for samples A through E, which are listed in Table I.

and bend deformations, and  $A\phi$  is torsional coupling strength. The  $d_e(1)$  represents a contribution originated from the effect of the spatial variation of the order parameter near the interface along the depth, and  $d_e(2)$  is the ordinary extrapolation length representing the contribution of the direct interaction at the interface that is called the intrinsic part. The meanings of these two lengths will be explained using the illustrations as follows. The conception of the extrapolation length that is generally accepted is shown in Figure 2(a). The abscissa expresses the direction of the normal to the substrate plane, where the plane of  $z = 0$  corresponds to the one side surface. The region where  $z > 0$  is the LC layer. For simplicity, only near the one side surface is illustrated. The ordinate expresses the azimuthal angle of the LC molecules from the easy axis. The LC molecules at the surface do not rotate when the torsional anchoring energy is infinite; for a finite external force, however, the molecules at the surface rotate by  $\phi_0$  when anchoring energy is finite. The spatial variation of the twist angle of LC molecules in the cell are shown by a solid line in the region of  $Z > 0$  in Figure 2(a). This line is extrapolated to the region of  $z < 0$ . The dotted line intersects with  $z$  axis at the point A. The length from the origin to the point A is defined as the extrapolation length  $d_e$  (actual length is  $d_e/2$ , but for simplicity we denote it as  $d_e$  for the moment).

Figure 2(b) illustrates the origins of three extrapolation lengths ( $d_e(1)$ ,  $d_e(2)$  and  $d_e$ ) in the case where  $S_s < S_b$ . If the surface order parameter  $S_s$  is smaller than the bulk order parameter  $S_b$ , which is a continuous function of the position, then the

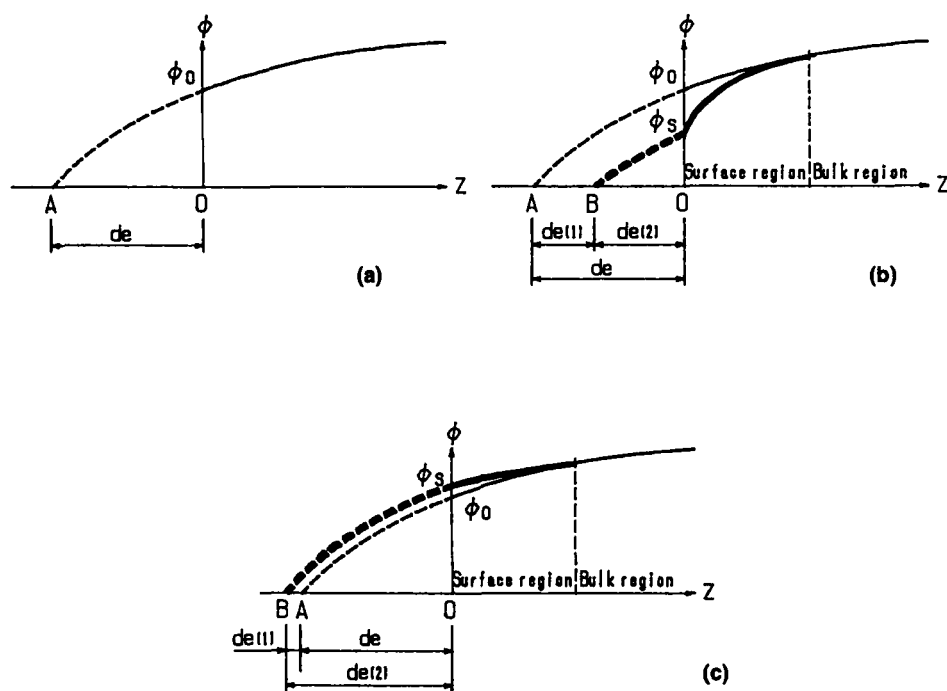


FIGURE 2 An illustrative drawing for three extrapolation lengths and the molecular conformation near one side surface in the case of  $S_s = S_b$ (a),  $S_s < S_b$ (b), and  $S_s > S_b$ (c).

elastic constant, which is in proportional to the square of the order parameter, has also a spatial variation that decreases with approaching to the surface. Consequently, the spatial variation of the LC molecular conformation is more rapid compared to the case where  $S_s = S_b$ . This conformation is expressed by the thick solid line in Figure 2(b). The intersection of this line and  $\phi$  axis is expressed by  $\phi_s$ . The region existing in the peculiar deformation is defined as the surface region. Another extrapolation is possible by approaching from a deep bulk region as expressed by a thin dotted line. Since the surface region is negligibly small compared to the bulk region,  $d_e$  which is obtained from the present macroscopical measurement is expressed by the extrapolation of the thin solid line. This extrapolated thin dotted line is shifted downward parallel to the intersect at  $\phi_s$ . This line is drawn by a thick dotted line, and it intersects with  $z$  axis at the point B. Then, the two lengths,  $d_e(1)$  and  $d_e(2)$  are given as illustrated in Figure 2(b), respectively. As is evident from the illustration, the relation between these three extrapolation lengths is,

$$d_e = d_e(1) + d_e(2). \quad (2)$$

Next, Figure 2(c) shows in the case of  $S_s > S_b$ . In this case, contrary to the above case, the deformation of the director is small when approaching the surface. In the same manner as Figure 2(b), there are two intersects (A and B). In this condition, three extrapolation lengths satisfy Equation (3):

$$d_e = (-d_e(1)) + d_e(2). \quad (3)$$

Then, it is found that  $d_e(1)$  has a plus or minus sign according to the relation between  $S_s$  and  $S_b$  in magnitude. Moreover, it is possible to consider that  $d_e(1) = 0$ , when  $S_s = S_b$ .

It is well known that the Frank elastic constant  $K_{ii}$  ( $i = 1, 2, 3$ ) is proportional to the square of the bulk order parameter  $S_b^2$ .<sup>8</sup>

Regarding the  $A\phi$ , various models have been proposed, among them a model based on the excluded volume effect<sup>9</sup> claims that the  $A\phi$  is proportional to  $kTS_s$ , where  $k$  and  $T$  stand for Boltzmann constant and absolute temperature, respectively, and another model based on van der Waals interaction<sup>10</sup> also claims the proportionality to  $S_s$ . However, we can neglect the effect of the variation of  $T$  in  $kTS_s$ , since it is just a few percent relative to room temperature expressed by  $K$ . Thus  $A\phi$  is safely assumed to be substantially proportional to  $S_s$  in both cases.

First, we try to discuss qualitatively by using these relations. There may be three different temperature variations of normalized  $S_s$  relative to that of  $S_b$  as follows: (case 1)  $S_s(T)/S_s = S_b(T)/S_b$ ; (case 2)  $S_s(T)/S_s > S_b(T)/S_b$ ; and (case 3)  $S_s(T)/S_s < S_b(T)/S_b$ , where the quantities of the dominators are the values at 25°C.

Because the sign of  $d_e(1)$  is not essentially important when the temperature dependence is considered, we restrict the plus sign in the present analysis. The temperature dependence of the molecular conformation near the surface and three extrapolation lengths for each case are shown in Figure 3. Each symbol is the same as those used in Figure 2, except for the extrapolation lengths at the high tem-

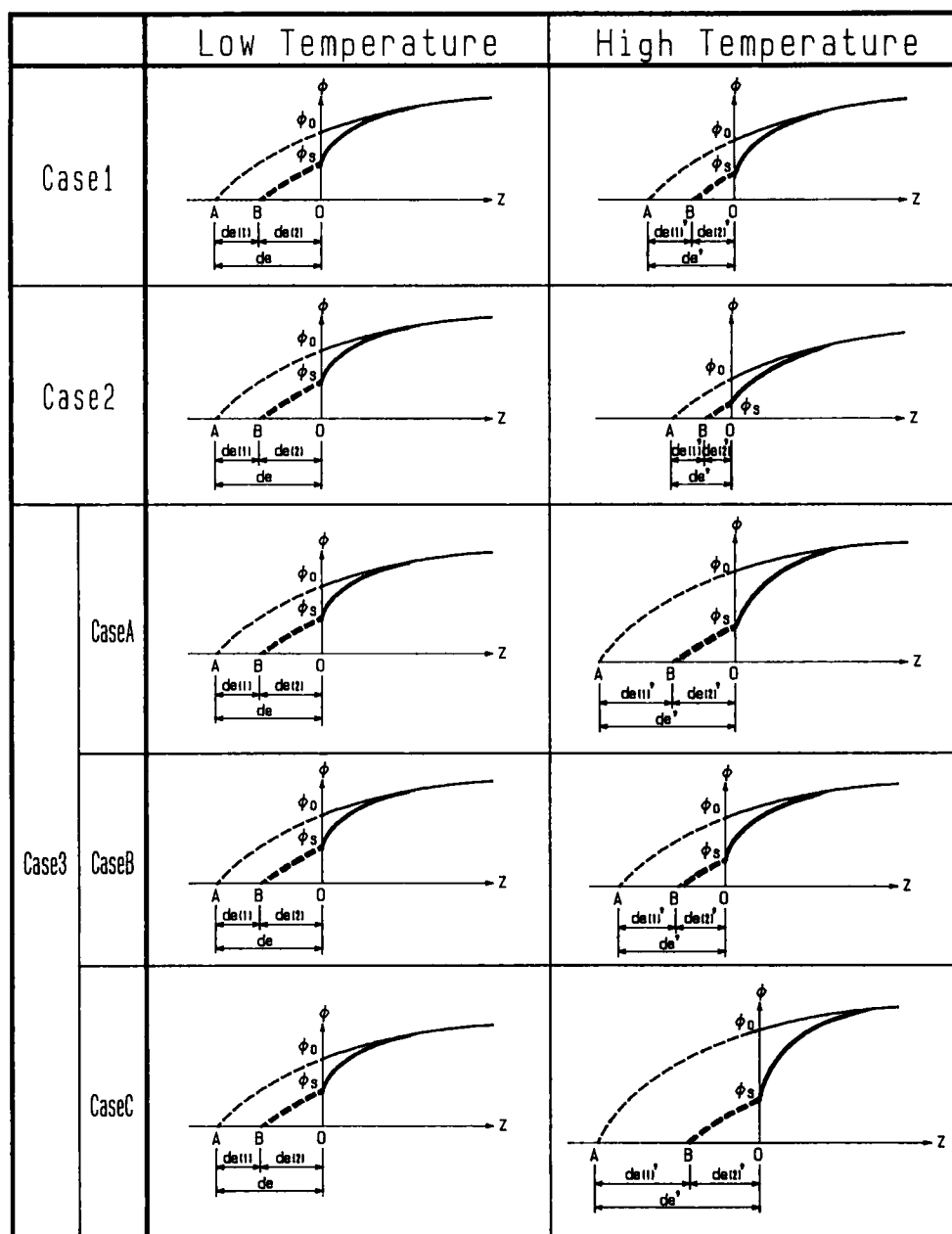


FIGURE 3 An illustrative drawing for the temperature variation of three extrapolation lengths and the molecular conformation near one side surface.

perature, which are distinguished by inserting primes. The temperature dependence of  $d_e(1)$ ,  $d_e(2)$ , and  $d_e$  in each case is discussed as follows. In case 1, the order parameter decreases with increasing temperature, but the relative spatial variation of it from the surface to the bulk remains constant for the relevant temperature



range, and the same is true for the Frank elastic constant. Then, the molecular conformation in the surface region does not change. Consequently,  $d_e(1)$  is constant regardless of the temperature. However,  $d_e(2)$  decreases in proportion to  $S_b$  with increasing temperature; this can be understood by substituting the above relation into Equation (1). By adding  $d_e(1)$  and  $d_e(2)$ , it is found that  $d_e$  decreases with increasing temperature. In case 2, the temperature variation of the Frank elastic constant near the surface becomes smaller compared with that of the bulk region because the relative spatial change of the order parameter does not remain constant, and thus the variation of the LC director becomes small when approaching the surface. So that  $d_e(1)$  decreases with increasing temperature, and  $d_e(2)$  also decreases;  $d_e(2)$  decreases more rapidly compared to case 1. Consequently,  $d_e$  decreases with increasing temperature. In case 3, contrary to case 2,  $d_e(1)$  increases with the temperature because the Frank elastic constant changes more rapidly near the surface. Thus the deformation of the molecular conformation is large when approaching the surface. When the temperature dependence of  $S_s$  is large,  $d_e(1)$  increases nearly divergently with the temperature. The  $d_e(2)$  is divided further into three cases by considering the relationship between the ratio of the temperature variation  $S_b^2(S_b^2(T)/S_b^2)$  and  $S_s(S_s(T)/S_s)$ : case A  $S_s(T)/S_s = S_b^2(T)/S_b^2$ ; case B  $S_s(T)/S_s > S_b^2(T)/S_b^2$ ; and case C  $S_s(T)/S_s < S_b^2(T)/S_b^2$ . So, as is evident from Equation (1),  $d_e(2)$  is constant, decreases, and increases with the increase of the temperature, in the order of cases A, B, and C, respectively. Consequently,  $d_e$  increases nearly divergently with the temperature when  $S_s(T)/S_s \leq S_b^2(T)/S_b^2$  (case A and C). Contrary to this, in the case of  $S_s(T)/S_s > S_b^2(T)/S_b^2$  (case B), the temperature dependence of  $d_e$  is decided by those relations. Thus,  $d_e$  becomes either the decreasing and increasing function with the temperature depending on the temperature dependence of  $d_e(1)$  and  $d_e(2)$ , moreover, according to circumstances, it may be the unchangeable function or have the maximum or minimum value. Table II summarizes the difference in the temperature dependence of  $d_e$ ,  $d_e(1)$ , and  $d_e(2)$  according to the five cases.

In the case where the PI films are used,  $d_e$  increases with the temperature but the amount of the change is small, so it can be considered that there is a relation between  $S_s$  and  $S_b$  that satisfies  $S_s(T)/S_s > S_b^2(T)/S_b^2$  (case B) in case 3. Accordingly,

TABLE II

		$d_e(1)$	$d_e(2)$	$d_e$
$S_s(T)/S_s = S_b(T)/S_b$		→	→	→
$S_s(T)/S_s > S_b(T)/S_b$		→	→	→
$S_s(T)/S_s < S_b(T)/S_b$	$S_s(T)/S_s = S_b^2(T)/S_b^2$	↗↗	→	↗↗
	$S_s(T)/S_s > S_b^2(T)/S_b^2$	↗	→	*
	$S_s(T)/S_s < S_b^2(T)/S_b^2$	↗↗	↗	↗↗

\*: ↗, →, or ↘ : it is decided by the relation between  $d_e(1)$  and  $d_e(2)$

it can be considered that the temperature variation of  $S_s$  is larger than that of  $S_b$  for PI films, but is not larger than that of  $S_b^2$ . In a cell with an obliquely evaporated SiO cell, because the temperature dependence of  $S_s$  is incomparably larger than that with PI films,  $d_e$  undergoes a diverging increase toward  $T_{NI}$ . This case is thought to satisfy the condition of  $S_s(T)/S_s \leq S_b^2(T)/S_b^2$  (cases A and C) in case 3. Anyway, it may be quite safe to say that the temperature variation of  $S_s$  for the SiO films is larger than that for PI films.

Second, we try to discuss more quantitatively. From the obtained value of  $d_e$  for PI cells, the values of  $d_e(1)$ ,  $d_e(2)$ , and these temperature variations are calculated based on the following four assumptions:

- 1) The  $d_e(1)$  is the same at the same temperature regardless of the existence of the branch and the pretilt angle.
- 2) The anchoring strength  $A\phi$  for the branched PI cell is divided into the two contributions: one is from the branch ( $A\phi(b)$ ), and the other is from the main chain of the orientation film ( $A\phi(m)$ ). And they satisfy the relation:  $A\phi = A\phi(b) + A\phi(m)$ .
- 3)  $A\phi$  for the branchless PI can be expressed only as  $A\phi(m)$ ; moreover, the  $A\phi(m)$  is the same regardless of the existence of the branch.
- 4)  $A\phi(b)$  is in proportion to the area of a triangle made by the branch,<sup>5</sup> where, the angle of the branch reflects the pretilt angle.

According to the above assumptions, Equation (1) can be rewritten as follows:

$$d_e = d_e(1) + g(\theta_0)/A\phi(m), \qquad \text{for branchless PI}$$
$$d_e = d_e(1) + g(\theta_0)/(A\phi(b) + A\phi(m)), \qquad \text{for branched PI}$$

(4)

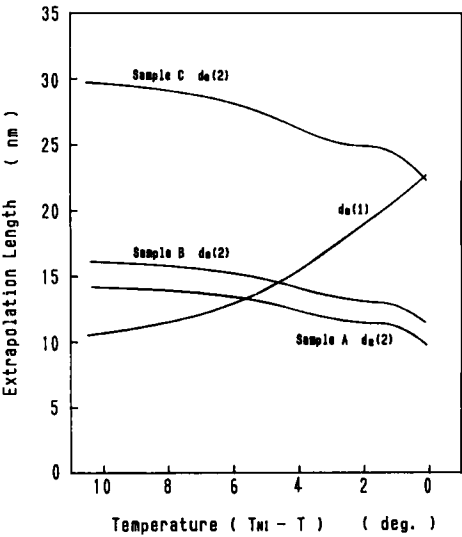


FIGURE 4 The result of the calculation of the temperature dependence of the divided extrapolation length  $d_e(1)$  and  $d_e(2)$  for samples A, B, and C. It is assumed that  $d_e(1)$  is the same for these three samples.

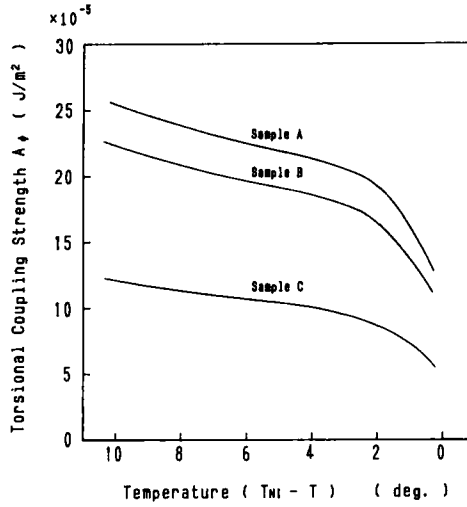


FIGURE 5 The result of the calculation of the temperature dependence of the torsional coupling strength for samples A, B, and C.

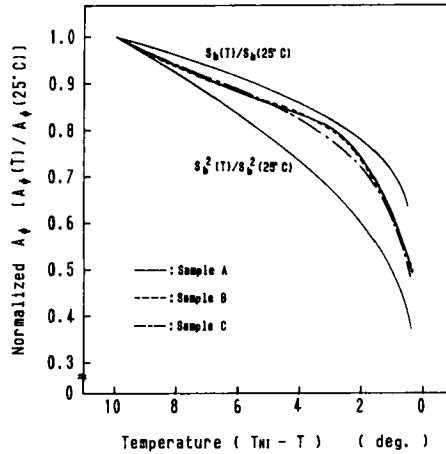


FIGURE 6 The comparison of the normalized torsional coupling strength with the normalized bulk order parameter and its square for samples A, B, and C.

Moreover, based on assumption (4),  $A\phi(b)$  can be written as

$$A\phi(b) \propto L_b^2 \sin \theta_0 \cos \theta_0 \quad (5)$$

where,  $L_b$  is the length of the branch.

The values of  $d_e(1)$ ,  $d_e(2)$ , and  $A\phi$  for each cell can be calculated by substituting each measurement value ( $d_e$ ,  $\phi_0$ ) into Equations (4) and (5). The results are shown in Figures 4 and 5. It is found from Figure 4 that  $d_e(1)$  increases with temperature, but  $d_e(2)$  decreases for all cells. It is equivalent to the condition  $S_s(T)/S_s > S_b^2(T)/S_b^2$ , which is mentioned in case 3 of the qualitative discussion. Consequently, for the PI cell it can be considered to satisfy  $S_b(T)/S_b > S_s(T)/S_s > S_b^2(T)/S_b^2$ .

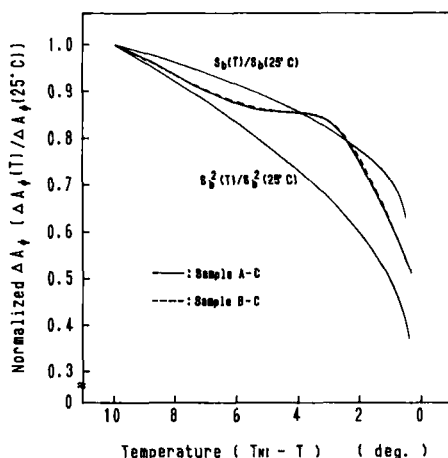


FIGURE 7 The comparison of the normalized extra torsional coupling strength with the normalized bulk order parameter and its square.

Moreover, the temperature variations of  $A\phi$  and  $\Delta A\phi$  normalized by the value at  $25^\circ\text{C}$  are shown in Figures 6 and 7, where  $\Delta A\phi$  is the extra torsional coupling strength which is mentioned in a previous paper.<sup>5</sup> It is found that the normalized values of  $A\phi$  and  $\Delta A\phi$  lie in the region between two lines which show  $S_b$  and  $S_b^2$  also normalized by each value at  $25^\circ\text{C}$ . Considering  $A\phi \propto S_s$ , these results may support our explanation mentioned in the qualitative discussion.

Finally, we will discuss the case where obliquely evaporated SiO films were used. Seo *et al.*<sup>11</sup> showed that the anchoring strength for the polar anchoring in the obliquely evaporated SiO cell is smaller than that for the rubbed PI cell (and hence the extrapolation length is larger); but regarding the torsional anchoring, it is shown, as is seen in Figure 1, that the value of  $d_e$  for the SiO cell is the same or rather small compared with that for a rubbed branchless PI cell. This may be explained by considering that there are large columns on the SiO surface that are responsible for resulting in a large  $A\phi$  owing to the steric interaction.

## 5. CONCLUDING REMARKS

The temperature dependences of the anchoring strength is analyzed by knowing the behavior of the surface order parameter. We measured the torsional anchoring strength which is shown to be nearly one or two orders smaller than that of the polar deformation. This situation makes the measurement easy. Through this research, we succeeded in devising a way to evaluate the temperature dependence of the surface order parameter, qualitatively. It is found, for polyimide films, that the temperature variation of  $S_s$  is larger than that of  $S_b$ , but smaller than that of  $S_b^2$ .

Moreover, in a quantitative analysis, the extrapolation length  $d_e$  is analyzed by dividing it into two contributions, ( $d_e(1)$  and  $d_e(2)$ ), and both values are evaluated separately. It is found that  $d_e(1)$  increases with the temperature, but contrary to

this  $d_e(2)$  decreases. These behaviors are in agreement with those obtained in our qualitative discussion.

As a point of reference, we investigated a cell with SiO films, and it is shown that the  $S_s$  for the SiO cell has a large temperature dependence in comparison with that for a PI cell.

## References

1. H. Yokoyama, S. Kobayashi and H. Kamei, *J. Appl. Phys.*, **61**, 4501 (1987).
2. H. Yokoyama and H. A. van Sprang, *J. Appl. Phys.*, **57**, 4520 (1985).
3. G. Haas, M. Fritsch, H. Wohler and D. A. Mlynski, *Liq. Cryst.*, **5**, 673 (1989).
4. L. M. Blinov, A. Yu. Kabayenkov and A. A. Sonin, *Liq. Cryst.*, **5**, 645 (1989).
5. T. Sugiyama, S. Kuniyasu, D. S. Seo, H. Fukuro and S. Kobayashi, *Jpn. J. Appl. Phys.*, **29**, 2045 (1990).
6. S. Faetti, M. Gatti, V. Palleschi and T. J. Sluckin, *Phys. Rev. Lett.*, **55**, 1681 (1985).
7. D. S. Seo, K. Muroi and S. Kobayashi, *Mol. Cryst. Liq. Cryst.*, **223**, 213 (1992).
8. G. Vertogen and W. H. de Jeu, "Thermotropic Liquid Crystals," Fundamentals, eds. Fritz P. Schafer (Springer-Verlag Berlin Heidelberg 1988) Chap. 6.
9. K. Okano, *Jpn. J. Appl. Phys.*, **22**, L343 (1983).
10. J. Bernasconi, S. Strassler and H. R. Zeller, *Phys. Rev.*, **A22**, 276 (1980).
11. D. S. Seo, K. Muroi, T. Isogami, H. Matsuda and S. Kobayashi, *Jpn. J. Appl. Phys.*, **31**, 2165 (1992).